Progressive Shrinkage of Involved Arteries in Parallel with Disease Progression in Moyamoya Disease

Shusuke Yamamoto[1], Daina Kashiwazaki[1], Naoki Akioka[1], Naoya Kuwayama[1], Kyo Noguchi[2], Satoshi Kuroda[1]

■ OBJECTIVE: **Recent three-dimensional constructive interference in steady state (3D-CISS) studies have shown that the involved arteries decrease not only their own luminal caliber but also outer diameter in moyamoya disease (MMD). This study was aimed to clarify how the outer diameter of the involved arteries serially change during disease progression in MMD using qunatitaive 3D-CISS imaging.**

■ METHODS: **This study included 8 hemispheres of 7 patients with MMD whose Suzuki angiographic stage spontaneously progressed during follow-up. Using 3D-CISS, the outer diameter was quantified serially in supraclinoid portion of internal carotid artery (C1), the horizontal portion of middle and anterior cerebral arteries (M1 and A1, respectively) before and after the spontaneous disease progression, and also 3–12 months later.**

■ RESULTS: **In 7 hemispheres with early disease stage (stage 1–3) at initial presentation, the involved arteries decreased in their outer dimater in parallel with luminal stenosis during spontaneous disease progression in the C1 ($P = 0.005$), M1 ($P < 0.0001$), and A1 portions ($P = 0.0048$). In the remaining 1 hemisphere with stage 4 at initial presentation, 3D-CISS imaging showed no significant change in the outer diameter of C1, M1, and A1 segments during disease progression.**

■ CONCLUSIONS: **Using quantitative 3D-CISS imaging, this study clearly shows that the involved arteries serially decrease in their own outer diameter in parallel with luminal stenosis during spontaneous disease progression in early stages of MMD (stage 1–3). This phenomenon has not been reported previously and may result from the pathognomic mechanisms underlying the development of MMD.**

INTRODUCTION

Moyamoya disease (MMD) is a unique cerebrovascular disorder characterized by progressive occlusion in the terminal portion of the internal carotid artery (ICA) and its main branches, the anterior cerebral artery, and middle cerebral artery (MCA). The diagnosis of MMD is based on the findings of cerebral angiography or magnetic resonance angiography (MRA), which means that the diagnosis completely depends on the narrowing of the internal lumen of the involved arteies.[1,2] As a result, it is often difficult to distiguish adult patients with MMD from those with intracranial arterial stenosis.[3,4] However, according to recent studies with noninvasive three-dimensional constructive interference in steady state (3D-CISS) imaging, the involved arteries also specifically decrease in their outer diameter as well as their internal caliber in MMD.[5-8] Kuroda et al.[7] reported that the outer diameter decreased in response to luminal stenosis in MMD but not in atherosclerotic M1 stenosis. Furthermore, the degree of this arterial shrinkage correlates well with the Suzuki angiographic stage. As a result, MMD may pathognomonically be characterized by both luminal stenosis and arterial shrinkage

Key words
- 3D-CISS
- Moyamoya disease
- Outer diameter

Abbreviations and Acronyms
3D-CISS: Three-dimensional constructive interference in steady state
BA: Basilar artery
EDMAPS: Encephaloduromyoarteriopericranial synangiosis
ICC: Intraclass correlation coefficient
ICA: Internal carotid artery
MCA: Middle cerebral artery
MMD: Moyamoya disease
MRA: Magnetic resonance angiography
MRI: Magnetic resonance imaging
PDGF: Platelet-derived growth factor
SAH: Subarachnoid hemorrhage
SPECT: Single-photon emission computed tomography
STA: Superficial temporal artery

From the Departments of [1]Neurosurgery and [2]Radiology, Graduate School of Medicine and Pharmaceutical Science, University of Toyama, Toyama, Japan

To whom correspondence should be addressed: Shusuke Yamamoto, M.D. [E-mail: s.yamamoto1007@gmail.com]

Citation: World Neurosurg. (2019) 122:e253-e261.
https://doi.org/10.1016/j.wneu.2018.10.001

*Journal homepage: **www.journals.elsevier.com/world-neurosurgery***

*Available online: **www.sciencedirect.com***

in a progressive fashion. On the other hand, a similar study has shown that patients with quasi-MMD (moyamoya syndrome) can be divided into at least 2 different subgroups: those with arterial shrinkage and those without.[3] This novel concept of arterial shrinkage is important in discussing the pathophysiology of MMD and reviewing the diagnosis criteria of MMD.

Based on these observations, this study aimed to clarify how the outer diameter of the involved artery serially changes during disease progression in MMD, using quantitative 3D-CISS imaging.

METHODS

Patients

Between March 2012 and December 2017, 92 patients were admitted to our hospital and were diagnosed with MMD. Of these patients, this study identified 8 hemispheres of 7 patients that met the following criteria: 1) bilateral-type MMD; 2) spontaneous disease progression during the follow-up period; and 3) 3D-CISS imaging before and after spontaneous disease progression. Spontaneous disease progression is defined as the progression of Suzuki angiographic stage in the nonoperated hemispheres[9] or that occurring in the operated hemispheres >1 year after surgery. There were 4 children and 3 adults. There were 2 males and 5 females. All were radiologically diagnosed with MMD based on the guideline for the diagnosis of MMD set by the Research Committee on Moyamoya Disease of the Ministry of Health, Welfare, and Labor of Japan.[1] As shown in Table 1, clinical diagnosis at initial presentation included transient ischemic attack in 5 patients and ischemic stroke in 2. Of these patients, 5 underwent superficial temporal artery (STA) to MCA anastomosis and encephaloduromyoarteriopericranial synangiosis

Table 1. Summary of Clinical Characteristics and Outer Diameter of Involved Arteries in 8 Hemispheres of 7 Patients with Moyamoya Disease

Case	Age (Years)/Sex	Diagnosis on Admission	Included Side	Examination Period	Suzuki Angiographic Stage	Outer Diameter (mm)			
						C1	M1	A1	Basilar Artery
1	14/F	TIA	R	Initial examination	1	2.9	1.7	1.7	3.1
				Just after progression	4	2.4	1.3	0.9	3.3
				5 months after progression	5	1.8	0.9	0.8	3.2
2	50/F	Ischemic stroke	L	Initial examination	4	2.5	1.3	1.2	2.8
				Just after progression	6	2.5	1.4	1.3	2.9
				6 months after progression	6	2.5	1.3	1.2	3.0
3	36/F	Ischemic stroke	L	Initial examination	3	2.6	1.8	1.1	2.5
				Just after progression	4	2.6	1.4	1.1	2.5
				4 months after progression	4	2.2	1.1	1.1	2.6
4	12/M	TIA	L	Initial examination	2	2.7	2.3	1.5	2.6
				Just after progression	4	2.2	1.7	1.5	2.7
				3 months after progression	5	1.8	1.0	1.1	2.7
5	8/M	TIA	L	Initial examination	1	2.7	1.9	1.0	2.9
				Just after progression	3	2.2	1.7	0.9	2.9
				6 months after progression	4	1.9	1.3	0.9	2.7
6	11/F	TIA	L	Initial examination	2	2.2	1.8	1.2	2.5
				Just after progression	3	2.3	1.7	1.2	2.3
				7 months after progression	3	2.3	1.1	0.9	2.5
7	6/M	TIA	R	Initial examination	3	1.9	1.7	1.6	2.5
				Just after progression	6	1.6	0.8	0.7	2.4
				4 months after progression	6	1.2	0.8	0.7	2.4
			L	Initial examination	2	2.4	2.1	1.5	2.5
				Just after progression	4	2.0	1.8	1.1	2.4
				8 months after progression	6	1.7	1.3	0.9	2.5

F, female; TIA, transient ischemic attack; R, right; L, left; M., male.

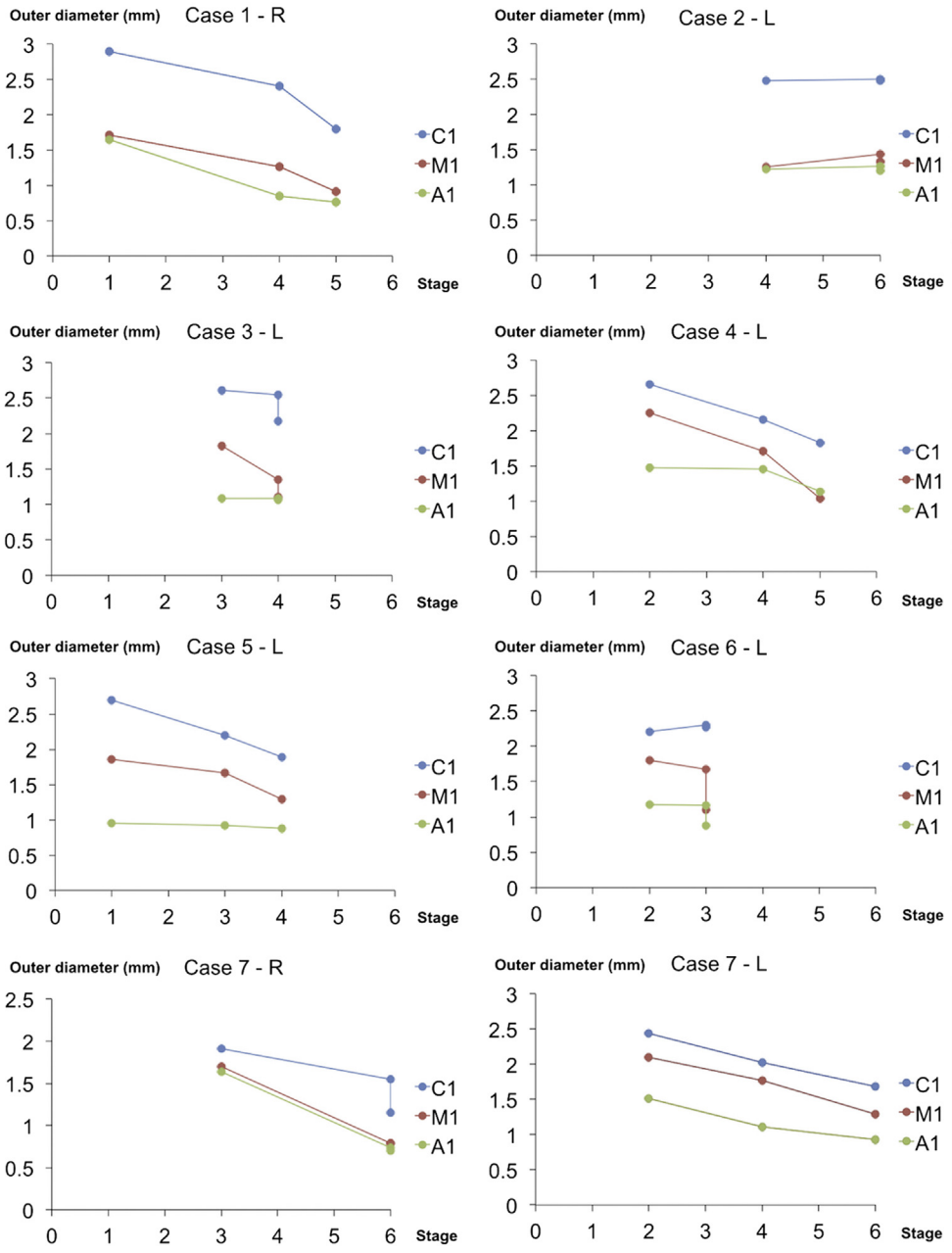

Figure 1. Plotted graphs show the serial change of outer diameters of C1, M1, and A1 portions associated with disease progression of Suzuki angiographic stage in 8 hemispheres. In all but 1 hemisphere with stage 4 at initial presentation (case 2), the outer diameters of ≥1 of 3 segments become smaller in parallel with progression of Suzuki angiographic stage. All 7 hemispheres were categorized into Suzuki stage 1–3 at initial presentation.

(EDMAPS) on the symptomatic side.[10] After surgery, the patients were medically followed up in the outpatient clinic, because the contralateral side was free from any cerebrovascular events. Serial MRA showed disease progression on the nonoperated hemisphere in all 5 patients during follow-up (cases 1, 2, 4, 5, and 6). Another patient was included in this study because the disease stage rapidly progressed on the symptomatic side when she was waiting for surgical revascularization (case 3). The remaining 1 patient who underwent STA-MCA anastomosis and EDMAPS on bilateral hemispheres was included because the disease stage bilaterally progressed at a

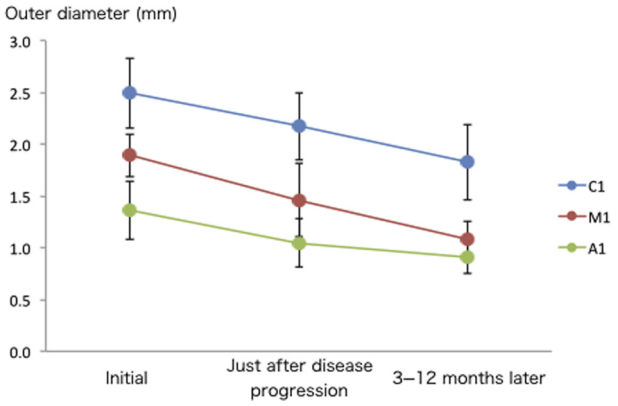

Figure 2. Plotted graph shows the serial changes of outer diameters of C1, M1, and A1 portions of 8 hemispheres. The bars represent standard deviation. All involved arteries decreased in their outer diameter during disease progression in a stepwise fashion.

long interval (<1 year) after STA-MCA anastomosis and EDMAPS on both sides (case 7). As a result, in this study, serial changes in the outer diameter were evaluated in 8 hemispheres of 7 patients before and after spontaneous disease progression (Table 1).

Radiologic Examinations

Magnetic resonance imaging (MRI), MRA, and cerebral angiography were performed in all 7 patients with MMD. MRI was obtained using a clinical 1.5-T or 3-T MRI unit (Magnetom Avanto or Verio [Siemens AG, Erlangen, Germany]) with a standard 12-channel head coil. T1-weighted images, T2-weighted images, T2*-weighted images, fluid-attenuated inversion recovery images, and diffusion-weighted images were obtained to locate ischemic and hemorrhagic lesions in the brain parenchyma. In this study, 3D-CISS images were obtained to evaluate the outer diameter of the intracranial arteries. Parameters for the 3D-CISS at 1.5 T were as follows: repetition time, 9.94 milliseconds; echo time, 4.97 milliseconds; flip angle, 70°; matrix size, 256 × 256; slice thickness, 0.7 mm; field of view, 160 mm; voxel size, 0.6 × 0.5 × 0.7 mm; number of excitations, 1: scan time, 4 minutes 16 seconds. Parameters for the 3D-CISS at 3 T were as follows: repetition time, 6.59 milliseconds; echo time, 2.77 milliseconds; flip angle, 40°; matrix size, 307 × 307; slice thickness, 0.6 mm; field of view, 160 mm; voxel size, 0.5 × 0.4 × 0.6 mm; number of excitations, 1: scan time, 4 minutes 24 seconds.[7] Using [^{123}I]-IMP single-photon emission computed tomography (SPECT), cerebral blood flow, and cerebrovascular reactivity to acetazolamide were also assessed on admission in all 7 patients.

Study Protocol

At initial presentation, the outer diameter of involved arteries was measured at the site where the outer diameter was smallest in the involved arteries before spontaneous disease progression. As a result, the outer diameter was quantified at the C1 segment just proximal to the bifurcation and at the M1 and A1 segments around 3–5 mm distal to the origins in most patients.[4] During follow-up, 3D-CISS imaging was repeated together with conventional MRI/MRA at 6-month intervals or when the patients developed any cerebrovascular events. Once spontaneous disease progression was identified on MRA or cerebral angiography during follow-up, the outer diameter was quantified again. Furthermore, 3D-CISS imaging with conventional MRI/MRA was repeated 3–12 months later after spontaneous disease progression was noted. As a result, 3D-CISS imaging was obtained 3 times in each patient. The outer diameter of the basilar artery (BA) was also quantified as the control in this study (Table 1). The outer diameter of C1, M1, A1, and BA was measured by 2 observers (S.Y. and D.K.).

Statistical Analysis

All data were expressed as mean ± standard deviaition. Continuous data were compared by 1-factor analysis of variance followed by a Tukey post hoc test among 3 groups. Values of $P < 0.05$ were considered statistically significant. The intraclass correlation coefficient (ICC) is a measure of the consistency of quantitative measurements made by 2 different observers and ranges from 0 (no association between the 2 measurements) to 1 (perfect agreement between the 2 measurements).

RESULTS

Radiologic Findings

On initial MRI, 7 of 8 hemispehres had neither cerebral infarction nor intracranial hemorrhage. The remaining 1 hemispehre had asymptomatic cerebral infarction. On initial cerebral angiography, the hemorrhages were graded as stage 1 in 2 hemispheres, stage 2 in 3, stage 3 in 2, and stage 4 in 1 according to Suzuki angiographic staging.

The findings on 3D-CISS imaging are summarized in Table 1. Of 6 nonoperated hemispheres (case 1–6), 5 developed cerebrovascular events during follow-up, including transient ischemic attack in 3 and ischemic stroke in 2 as a result of spontaneous disease progression. Disease progression was noted on follow-up MRI/MRA without any cerebrovascular event in the remaining 1 hemisphere. Two operated hemispheres (case 7) developed no cerebrovascular events after surgical revascularization and disease progression was noted on follow-up MRI/MRA. Suzuki angiographic stage advanced to stage 3 in 2 hemispheres, stage 4 in 3, stage 5 in one, and stage 6 in 2.

Outer Diameter Change During Disease Progression

Using 3D-CISS, the outer diameter of involved arteries (C1, M1, and A1 segments) was serially quantified in 8 hemispheres before and after spontaneous disease progression (Table 1). The ICC was 0.896 between the 2 observers. This high ICC value shows excellent agreement between the 2 observers in measurement of outer diameter of C1, M1, A1, and BA using 3D-CISS. In all but 1 patient with stage 4 at initial presentation (case 2), the outer diameter of ≥1 of 3 segments decreased in response to spontaneous disease progression (Table 1, Figure 1). All 7 hemispheres were categorized into Suzuki stage 1–3 at initial presentation. The outer diameter of their C1, M1, and A1 segements was quantitatively determined before, just after, and several months after spontaneous disease progression. As shown in Figure 2, the outer diameter of their C1 segment decreased from 2.49 ± 0.33

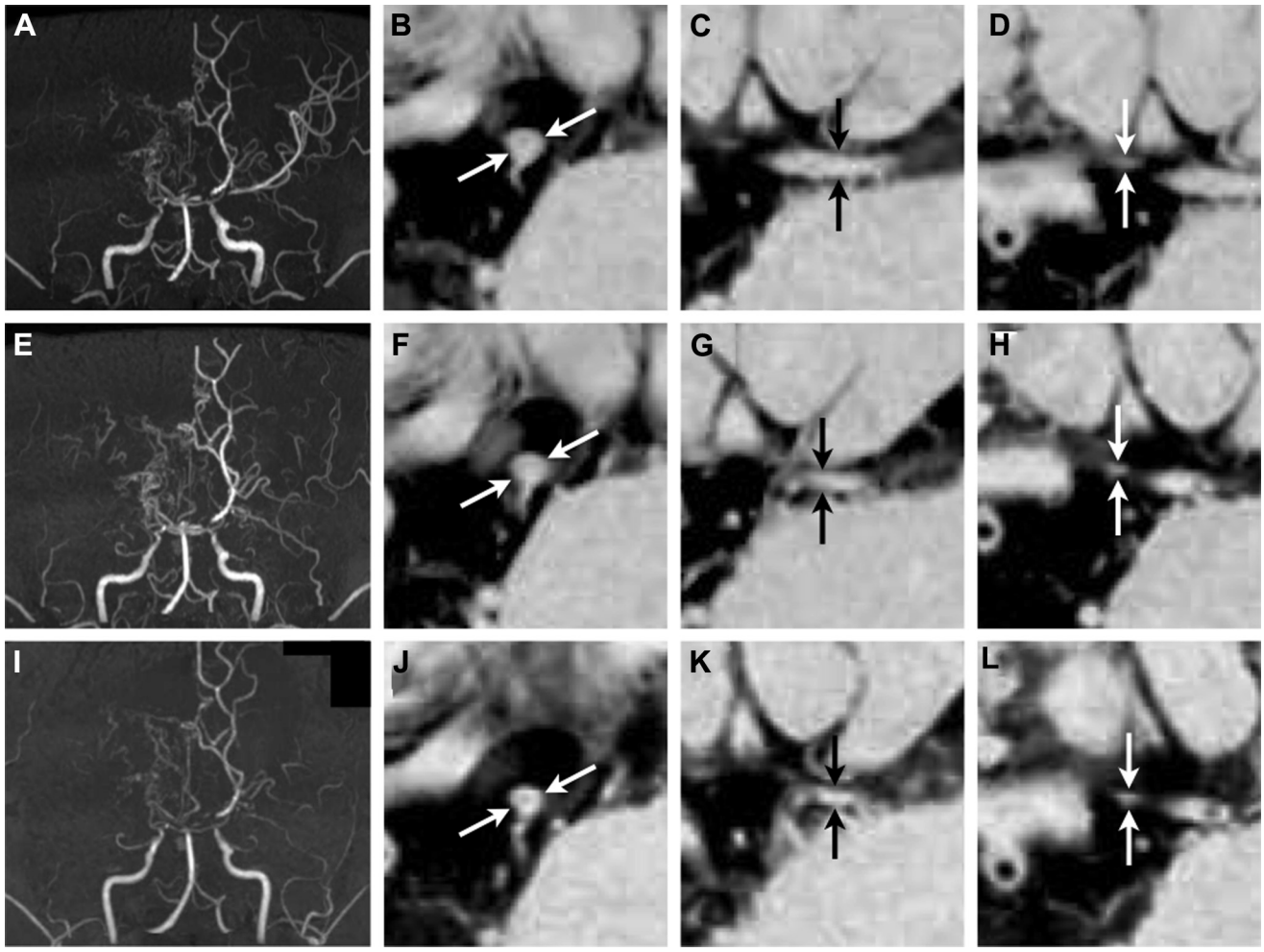

Figure 3. Serial magnetic resonance angiography (MRA) (**A**, **E**, **I**) and three-dimensional constructive interference in steady state (3D-CISS) imaging (**B**–**D**, **F**–**H**, **J**–**L**) of 36-year-old woman with bilateral moyamoya disease (MMD) with ischemic stroke in left frontal cortex (case 3). (**A**) On MRA at initial presentation, the internal carotid artery (ICA) is occluded on the right side and the terminal portion of the ICA (C1) to proximal portion of the middle cerebral artery (MCA) (M1) is severely stenosed and the anterior cerebral artery is occluded on the left side, graded as stage 5 and 3, respectively. On 3D-CISS imaging at initial presentation, the outer diameters of C1 (**B**), M1 (**C**), and A1 (**D**) on the left side are 2.61, 1.83, and 1.09 mm, respectively (*arrows*). (**E**) On MRA performed just after spontaneous progression of disease stage on the left side, the ICA is occluded on the left side, graded as stage 4 on the left side. On 3D-CISS imaging performed just after progression of disease stage on the left side, the outer diameters of C1 (**F**), M1 (**G**), and A1 (**H**) are 2.55, 1.35, and 1.09 mm, respectively (*arrows*). (**I**) On MRA performed 2 months after the progression of disease stage on the left side, no further disease progression is seen, graded as stage 4 on the left side. On 3D-CISS imaging performed 2 months after the progression of disease stage on the left side, the outer diameters of C1 (**J**), M1 (**K**), and A1 (**L**) are 2.18, 1.11, and 1.06 mm, respectively (*arrows*).

mm to 2.17 ± 0.32 mm ($P = 0.22$), and then to 1.83 ± 0.37 mm ($P = 0.005$). The difference between the initial and final examinations was 0.66 ± 0.37 mm. The outer diameter of their M1 segment decreased from 1.89 ± 0.21 mm to 1.46 ± 0.35 mm ($P = 0.015$), and then further decreased to 1.08 ± 0.18 mm ($P < 0.0001$). The difference between the initial and final examinations was 0.82 ± 0.20 mm. The outer diameter of their A1 segment decreased from 1.36 ± 0.28 mm to 1.05 ± 0.24 mm ($P = 0.052$) and then further decreased to 0.91 ± 0.15 mm ($P = 0.0048$). The difference between the initial and final examinations was 0.45 ± 0.37 mm. Therefore, the involved arteries decreased in their outer diameter in parallel with spontaneous disease progression. Representative cases are shown in Figures 3 and 4.

As shown in Figure 1, the involved arteries further decreased in their outer diameter between the second and third examination in 3 of 8 hemispheres, although their disease stage did not change for the same period (case 3-L, case 6-L, and case 7-R).

In the remaining patient with stage 4 at initial presentation (case 2), 3D-CISS imaging showed no significant change in the outer diameter of C1, M1, and A1 segment (Figure 1). In addition, the outer diameter of the BA showed no significant change in this study in all 7 patients (Table 1).

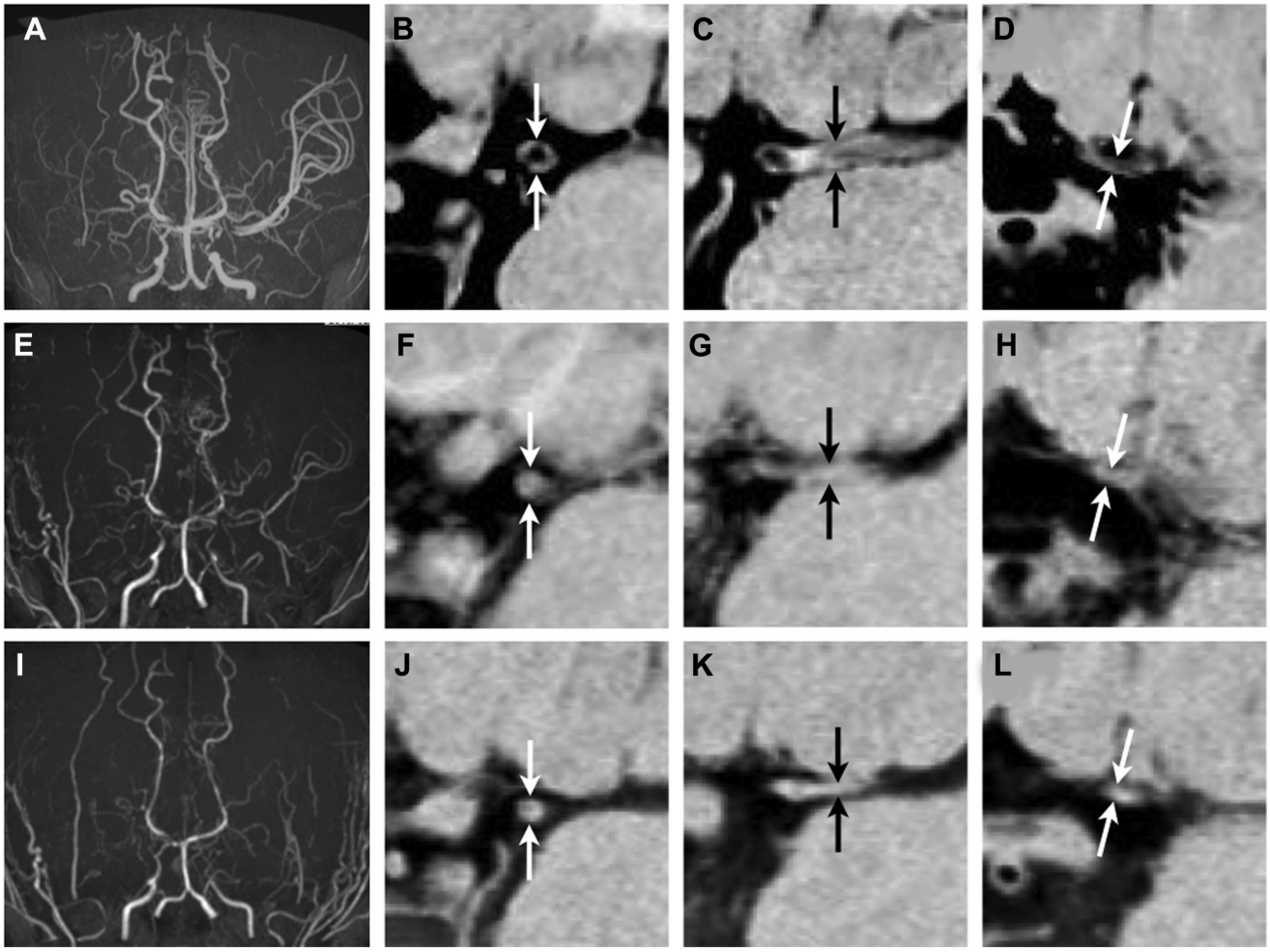

Figure 4. Serial magnetic resonance angiography (MRA) (**A, E, I**) and 3D-CISS imaging (**B**–**D, F**–**H, J**–**L**) of 12-year-old boy with bilateral moyamoya disease with transient ischemic attack (case 4). (**A**) On MRA at initial presentation, the internal carotid artery (ICA) is occluded on the right side, graded as stage 4. The terminal portion of the ICA to the proximal portion of the middle cerebral artery (MCA) and anterior cerebral artery (ACA) are severely stenosed but the distal parts of the MCA and ACA are opacified on the left side, graded as stage 2. On three-dimensional constructive interference in steady state (3D-CISS) imaging at initial presentation, the outer diameters of C1 (**B**), M1 (**C**), and A1 (**D**) on the left side are 2.66, 2.25, and 1.48 mm, respectively (*arrows*). (**E**) On MRA performed just after spontaneous progression of disease stage on the left side, the terminal portion of the ICA to the proximal portion of the MCA is severely stenosed and the ACA is occluded on the left side, graded as stage 4 on the left side. On 3D-CISS imaging performed just after progression of disease stage on the left side, the outer diameters of C1 (**F**), M1 (**G**), and A1 (**H**) are 2.16, 1.71, and 1.45 mm, respectively (*arrows*). (**I**) On MRA performed 4 months after the progression of disease stage on the left side, further disease progression is seen, graded as stage 5 on the left side. On 3D-CISS imaging performed 4 months after the progression of disease stage on the left side, the outer diameters of C1 (**J**), M1 (**K**), and A1 (**L**) are 1.83, 1.04, and 1.14 mm, respectively (*arrows*).

In all 8 hemispheres of 7 patients, cerebral blood flow and cerebrovascular reactivity to acetazolamide were assessed on admission using [^{123}I]-IMP SPECT. In all 8 hemispheres of 7 patients, [^{123}I]-IMP SPECT showed impaired cerebral blood flow and reactivity to acetazolamide in the territory of the involved ICA or MCA. There was no correlation between cerebral blood flow and outer diameter of involved arteries.

Treatments and Prognosis

All of 6 nonoperated hemispheres underwent STA-MCA anastomosis and EDMAPS after spontaneous disease progression. Postoperative courses were uneventful. The courses of the remaining 2 hemispheres that had already undergone STA-MCA anastomosis and EDMAPS were also uneventful. None developed any iscehmic or hemorrhagic stroke after surgery. Follow-up cerebral angiography performed 4–6 months after surgery showed well-developed surgical collaterals through both direct and indirect bypass in all 8 hemispheres.

DISCUSSION

As discussed, the main aim of this study was to clarify the relationship between the spontaneous progression of disease stage and

the change in the outer diameter of involved arteries in MMD. In this study, 1 patient who underwent STA-MCA anastomosis and EDMAPS on bilateral hemispheres (case 7) was included, because the disease stage bilaterally progressed at a long interval (>1 year) after STA-MCA anastomosis and EDMAPS on both sides. In a previous study,[11] it was reported that indirect bypass through the deep temporal artery or middle meningeal artery develops within 3 months in most cases. The progression of stenotic change in the carotid fork is accelerated after surgery and appears 3–6 months after surgery. Therefore, we speculated that the progression of stenotic lesion in the carotid fork of case 7 occurred spontaneously. As a result, this study clearly shows that the involved arteries decrease their own outer diameter in parallel with disease progression in 7/8 hemispheres with early disease stage (stage 1–3) at initial presentation. Such changes in the involved artery were not observed in the remaining 1 hemisphere with stage 4 at initial presentation. These findings strongly suggest that the arterial shrinkage progresses as luminal stenosis is advanced. This is the first report showing serial shrinkage of the involved arteries during disease progression in MMD by serially observing their outer diameter on 3D-CISS imaging. This phenomenon may result from progressive pathophysiologic change of involved arteries in MMD. MMD has pathognomonic fingings in the carotid fork, including fibrocellular thickening of the intima, an irregular undulation (waving) of the internal elastic lamina, and attenuation of the media.[12,13] Intimal thickening should directly lead to narrowing of the arterial lumen. On the other hand, the attenuation of the media may decrease the volume of the arterial wall, causing narrowing of the outer diameter. Therefore, the present results strongly suggest that degeneration of media progresses in parallel with progressive intimal thickening in the early stage of MMD and irregular waving may be accompanied by this arterial shrinkage specific for MMD (Figure 5). A similar phenomenon has also been observed previously in vasospasm. Uchida et al.[14] established an animal model of coronary artery spasm in the beagle and found that the internal elastic lamina were markedly folded like the "bellows of an old-fashioned camera." Based on their results, these investigators hypothetized that this phenomenon would play an essential role in coronary artery spasm, which caused narrowing of the outer diameter. Furthermore, Sakaki et al.[15] evaluated the pathologic findings of cerebral vasospasm caused by aneurysmal subarachnoid hemorrhage (SAH) and reported that the cerebral arterial wall corresponding to the angiographic vasospasm showed various structural changes. The changes were divided into 5 groups as follows: in group 1, the intraluminal size of the arterial wall was reduced with medial thickening, marked waving of the internal elastic lamina, and intimal edema; in group 2, the necrosis of the smooth muscle cells in the media, partial break of internal elastic lamina, and the profuse deposition of acid mucopoly saccharides were observed; in group 3, marked intimal thickening and medial atrophy were seen; in group 4, a dilatation of luminal size with improvement of the intimal thickening and remarkable medial atrophy were noted; and in group 5, regeneration of smooth muscle cell in the media was observed. Histopathologic change seen in group 3, including intimal thickening and medial atrophy, may be similar to that observed in the carotid fork of MMD. Sakaki et al.[15] speculated that medial atrophy resulted from the necrosis of smooth muscle cells followed by replacement with collagen fiber. In addition, Takagi et al.[16] accessed the arterial wall of the cortical branch of MCA during bypass surgery for MMD and found that the media in the MCA developed

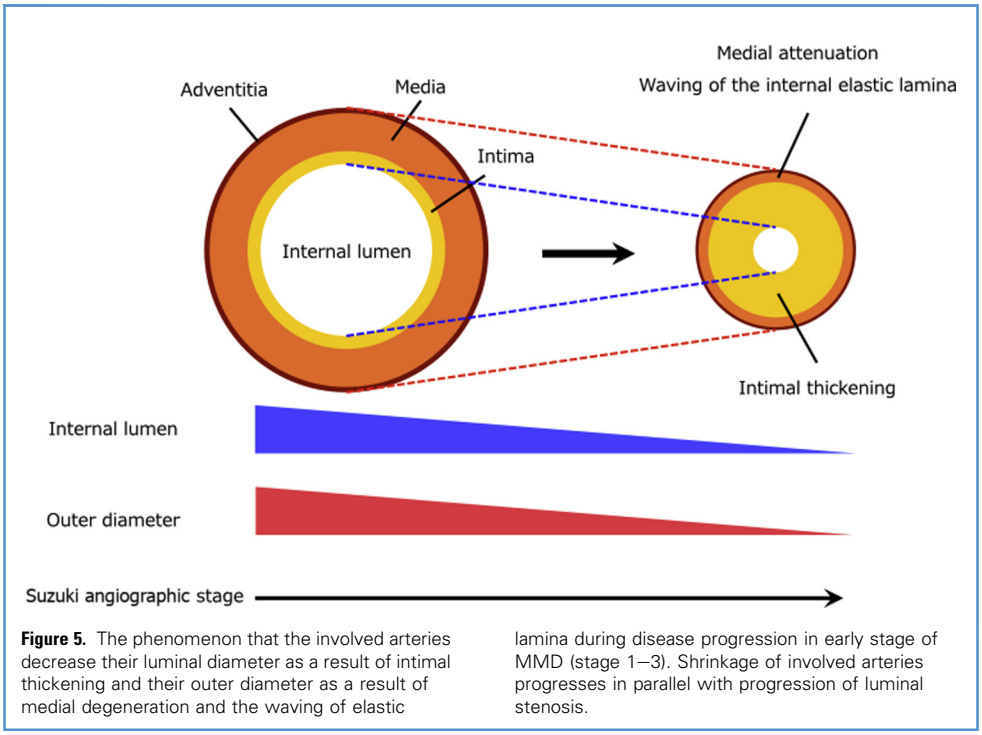

Figure 5. The phenomenon that the involved arteries decrease their luminal diameter as a result of intimal thickening and their outer diameter as a result of medial degeneration and the waving of elastic lamina during disease progression in early stage of MMD (stage 1–3). Shrinkage of involved arteries progresses in parallel with progression of luminal stenosis.

caspase-3-induced apoptosis. Medial degeneration and waving of elastic lamina may be common pathologic findings in MMD and arterial vasospasm. Recent studies have shown that a subgroup of patients with intracranial major artery stenosis have a common genetic variant, ring finger 213 (RNF 213) c.14576G>A, known as a susceptibility gene for MMD.[17] On the other hand, several studies have reported the role of genetic polymorphisms in cerebral vasospasm after aneurysmal SAH. Haptoglobin genotype 2-2 has been reported to have strong associations with focal and global cerebrovasospasm after aneurysmal SAH and also to predict poor functional outcomes and mortality.[18] The association between apolipoprotein E4 and cerebral vasospasm has previously been observed in rodent models.[19] Past studies have reported that platelet-derived growth factor (PDGF)-β associates with cerebral vasospasm; furthermore, the degree of vessel stenosis directly correlates with the temporal expression dynamics of PDGF-β, as shown in a rabbit model of SAH.[20] In human patients with SAH, higher PDGF levels predict greater probability of developing cerebral vasospasm.[21-23] Considering that arterial shrinkage is a specific finding in MMD and a similar phenomenon has been recognized in cerebral vasospasm, such genetic variants or polymorphisms may play a key role in clarifying the cause of shrinkage in the involved arteries in MMD.

In addition, this study shows that the involved arteries further decrease in their outer diameter between the second and third examination in 3 of 8 hemispheres, although their disease stage does not change for the same period (**Figure 1**). The finding strongly suggests that disease progression may occur in a step-by-step fashion in MMD; intimal thickening may first lead to luminal stenosis and then medial atrophy may cause arterial shrinkage.

There are some limitaions to this study. First, the sample size is small ($n = 8$) to reach a final conclusion about pathophysiologic mechanisms in MMD. Therefore, further studies with larger cohorts are warranted to confirm the present results. Second, intra-observer variability was not evaluated in this study. Therefore, this factor should also be analyzed in the future multicenter cohort studies.

CONCLUSIONS

Using quantitative 3D-CISS imaging, this study clearly shows that the involved arteries decrease their outer diameter serially in parallel with progressive luminal stenosis during disease progression in the early stage of MMD (stage 1–3). This phenomenon has not reported before and may result from pathophysiologic mechanisms underlying the development of MMD.

REFERENCES

1. Research Committee on the Pathology and Treatment of Spontaneous Occlusion of the Circle of Willis; Health Labour Sciences Research Grant for Research on Measures for Infractable Diseases. Guidelines for diagnosis and treatment of moyamoya disease (spontaneous occlusion of the circle of Willis). *Neurol Med Chir*. 2012;52:245-266.

2. Suzuki J, Takaku A. Cerebrovascular "moyamoya" disease. Disease showing abnormal net-like vessels in base of brain. *Arch Neurol*. 1969;20:288-299.

3. Yamamoto S, Koh M, Kashiwazaki D, Akioka N, Kuwayama N, Noguchi K, et al. Is Quasi-moyamoya Disease a Uniform Disease Entity? A Three-Dimensional Constructive Interference in Steady State Imaging Study. *J Stroke Cerebrovasc Dis*. 2016;25:1509-1516.

4. Miyawaki S, Imai H, Takayanagi S, Mukasa A, Nakatomi H, Saito N. Identification of a genetic variant common to moyamoya disease and intracranial major artery stenosis/occlusion. *Stroke*. 2012;43:3371-3374.

5. Kaku Y, Morioka M, Ohmori Y, Kawano T, Kai Y, Fukuoka H, et al. Outer-diameter narrowing of the internal carotid and middle cerebral arteries in moyamoya disease detected on 3D constructive interference in steady-state MR image: is arterial constrictive remodeling a major pathogenesis? *Acta Neurochir (Wien)*. 2012;154:2151-2157.

6. Kim YJ, Lee DH, Kwon JY, Kang DW, Suh DC, Kim JS, et al. High resolution MRI difference between moyamoya disease and intracranial atherosclerosis. *Eur J Neurol*. 2013;20:1311-1318.

7. Kuroda S, Kashiwazaki D, Akioka N, Koh M, Hori E, Nishikata M, et al. Specific shrinkage of carotid forks in moyamoya disease: a novel key finding for diagnosis. *Neurol Med Chir (Tokyo)*. 2015;55:796-804.

8. Ryoo S, Cha J, Kim SJ, Choi JW, Ki CS, Kim KH, et al. High-resolution magnetic resonance wall imaging findings of Moyamoya disease. *Stroke*. 2014;45:2457-2460.

9. Kuroda S, Ishikawa T, Houkin K, Nanba R, Hokari M, Iwasaki Y. Incidence and clinical features of disease progression in adult moyamoya disease. *Stroke*. 2005;36:2148-2153.

10. Kuroda S, Houkin K, Ishikawa T, Nakayama N, Iwasaki Y. Novel bypass surgery for moyamoya disease using pericranial flap: its impacts on cerebral hemodynamics and long-term outcome. *Neurosurgery*. 2010;66:1093-1101 [discussion: 1101].

11. Houkin K, Nakayama N, Kuroda S, Ishikawa T, Nonaka T. How does angiogenesis develop in pediatric moyamoya disease after surgery? A prospective study with MR angiography. *Childs Nerv Syst*. 2004;20:734-741.

12. Haltia M, Iivanainen M, Majuri H, Puranen M. Spontaneous occlusion of the circle of Willis (moyamoya syndrome). *Clin Neuropathol*. 1982;1:11-22.

13. Coakham HM, Duchen LW, Scaravilli F. Moyamoya disease: clinical and pathological report of a case with associated myopathy. *J Neurol Neurosurg Psychiatry*. 1979;42:289-297.

14. Uchida Y, Uchida Y, Matsuyama A, Koga A, Maezawa Y, Maezawa Y, et al. Functional medial thickening and folding of the internal elastic lamina in coronary spasm. *Am J Physiol Heart Circ Physiol*. 2011;300:H423-H430.

15. Sakaki T, Tanigake T, Kyoi K, Utumi S, Murata Y, Hiasa Y, et al. [Pathological study of late arterial spasm (author's transl)]. *Neurol Med Chir (Tokyo)*. 1979;19:1085-1093 [in Japanese].

16. Takagi Y, Kikuta K, Sadamasa N, Nozaki K, Hashimoto N. Caspase-3-dependent apoptosis in middle cerebral arteries in patients with moyamoya disease. *Neurosurgery*. 2006;59:894-900 [discussion: 900-901].

17. Miyawaki S, Imai H, Shimizu M, Yagi S, Ono H, Mukasa A, et al. Genetic variant RNF213 c.14576G>A in various phenotypes of intracranial major artery stenosis/occlusion. *Stroke*. 2013;44:2894-2897.

18. Leclerc JL, Blackburn S, Neal D, Mendez NV, Wharton JA, Waters MF, et al. Haptoglobin phenotype predicts the development of focal and global cerebral vasospasm and may influence outcomes after aneurysmal subarachnoid hemorrhage. *Proc Natl Acad Sci U S A*. 2015;112:1155-1160.

19. Gao J, Wang H, Sheng H, Lynch JR, Warner DS, Durham L, et al. A novel apoE-derived therapeutic reduces vasospasm and improves outcome in a murine model of subarachnoid hemorrhage. *Neurocrit Care*. 2006;4:25-31.

20. Cui H-K, Yan RF, Ding XL, Zhao P, Wu QW, Wang HP, et al. Platelet-derived growth factor-beta expression in rabbit models of cerebral vasospasm following subarachnoid hemorrhage. *Mol Med Rep*. 2014;10:1416-1422.

21. Gaetani P, Tancioni F, Grignani G, Tartara F, Merlo EM, Brocchieri A, et al. Platelet derived growth factor and subarachnoid haemorrage: a

study on cisternal cerebrospinal fluid. *Acta Neurochir (Wien)*. 1997;139:319-324.

22. Lad SP, Hegen H, Gupta G, Deisenhammer F, Steinberg GK. Proteomic biomarker discovery in cerebrospinal fluid for cerebral vasospasm following subarachnoid hemorrhage. *J Stroke Cerebrovasc Dis*. 2012;21:30-41.

23. Yanamoto H, Kataoka H, Nakajo Y, Iihara K. The role of the host defense system in the development of cerebral vasospasm: analogies between atherosclerosis and subarachnoid hemorrhage. *Eur Neurol*. 2012;68:329-343.

Conflict of interest statement: This study was supported by a grant from the Research Committee on Moyamoya Disease, sponsored by the Ministry of Health, Labor, and Welfare of Japan.

Received 11 June 2018; accepted 1 October 2018

Citation: World Neurosurg. (2019) 122:e253-e261.
https://doi.org/10.1016/j.wneu.2018.10.001

Journal homepage: ***www.journals.elsevier.com/world-neurosurgery***

Available online: ***www.sciencedirect.com***

1878-8750/$ - see front matter